Atomic layer deposition of Al_2O_3 and TiO_2 multilayers for applications as bandpass filters and antireflection coatings

Adriana Szeghalmi,[1] Michael Helgert,[2] Robert Brunner,[2] Frank Heyroth,[3] Ulrich Gösele,[1] and Mato Knez[1,*]

[1]Max Planck Institute of Microstructure Physics, Weinberg 2, D-06120 Halle (Saale), Germany

[2]Carl Zeiss GmbH, Carl-Zeiss-Promenade 10, D-07745 Jena, Germany

[3]Martin-Luther University Halle-Wittenberg, Heinrich-Damerow Str. 4, D-06120 Halle (Saale), Germany

*Corresponding author: mknez@mpi-halle.de

Received 6 January 2009; revised 3 March 2009; accepted 3 March 2009; posted 4 March 2009 (Doc. ID 106079); published 13 March 2009

Al_2O_3 and TiO_2 thin films have been deposited on Si wafers, quartz, BK7 glass, and polycarbonate substrates by atomic layer deposition (ALD). The refractive indices and growth rates of the materials have been determined by spectroscopic ellipsometry and transmission electron microscopy. The influence of substrate temperature and precursor on the refractive indices has been investigated. The refractive index of TiO_2 significantly increases with temperature, whereas the Al_2O_3 films are temperature insensitive. The films deposited using H_2O_2 as oxygen source show a slightly higher refractive index than the films prepared with H_2O. Multilayer narrow-bandpass filters and broadband antireflective coatings have been designed and produced by ALD. © 2009 Optical Society of America

OCIS codes: 310.0310, 310.1210, 310.1620, 310.1860, 310.4165.

1. Introduction

Dielectric thin-film-based multilayer coatings are widely used in optics and electronics. Various coating technologies, such as chemical vapor deposition (CVD), physical vapor deposition (PVD), ion beam sputtering, magnetron reactive sputtering, and plasma-ion-assisted deposition, are currently applied [1–5]. Atomic layer deposition (ALD) is similar to CVD, however, with marking differences [6,7]. The reactants are introduced into the reaction chamber successively, and the reaction is surface controlled with the film growing with a (sub)monolayer thickness per cycle. Hence ALD has received increasing interest as coating technology, because it offers tight control of the film thickness [6,7]. Additionally, ALD of various dielectric material films is possible at low substrate temperatures (below 200 °C), making it interesting for coating polymers.

The design of optical coatings such as filters and antireflective coatings based on multilayer systems requires detailed knowledge of the optical properties of the materials. The dispersion curves and the growth rates of the dielectric films must be accurately determined. Unfortunately, several factors will affect these properties. The deposition technique and conditions (e.g., temperature and pressure) uniquely determine the characteristics of the films [4]. *In situ* monitoring of the film growth based on complex simulation algorithms are generally applied to produce specialty optics [8–10]. Even under tight *in situ* control, it is difficult to technically meet stringent tolerances.

We present a thorough characterization of Al_2O_3 and TiO_2 thin films deposited by ALD using spectroscopic ellipsometry, x-ray reflectometry, and transmission electron microscopy (TEM). The films were

0003-6935/09/091727-06$15.00/0
© 2009 Optical Society of America

grown on silicon wafer, BK7 glass, polycarbonate (PC), quartz, and poly(methyl methacrylate) substrates. The films were deposited in the 80–200 °C temperature range, and the changes in refractive indices and growth rates were determined. Multilayer coatings for narrow-bandpass filters (NBPFs) and antireflection coatings using ALD are demonstrated, whereby the target is achieved without *in situ* monitoring.

2. Experiment

A. Atomic Layer Deposition

Deposition of thin Al_2O_3 and TiO_2 layers was carried out in a commercial hot-wall flow-type ALD reactor (SUNALE R75, Picosun, Finland). Trimethylaluminum [$Al(CH_3)_3$ (TMA)], titanium(IV) isopropoxide ($Ti[OCH(CH_3)_2]_4$ [TiOP]) and H_2O or 30% H_2O_2 were used as aluminum, titanium, and oxygen reactant sources, respectively. The TiOP precursor was heated to 45–60 °C and delivered through a booster system. The pulsing times were 0.1 s for TMA, 0.5 s for TiOP, and 2 s for H_2O or H_2O_2 with N_2 as carrier gas at a flow rate of 200 sccm (sccm denotes cubic centimeters per minute at standard temperature and pressure). The purging time after each pulse was set to 4 s. Purging was done with N_2 gas with a flow rate of 200 sccm.

B. Ellipsometry

Spectroscopic ellipsometry measurements in the 370–1000 nm spectral range were done with a J. A. Woollam M2000 ellipsometer equipped with a rotating analyzer and a compensator. The experimental data were analyzed with the WVase32 software provided with the equipment. Transmittance spectra were recorded with the Woollam M2000 equipment and with a NanoCalc 2000 spectrometer. The spectral range of the spectrometer was 280–850 nm; the UV VIS–NIR source and the transmitted light were coupled by optical fibers to the detector. Background spectra were recorded prior and after the transmittance measurements to assure no intensity variation of the incident light.

C. Coating Design

Coating designs were calculated using commercially available software (IMD). An ideal model without surface roughness was applied. The effect of thickness variation of individual layers on the optical performance of the NBPF has been evaluated.

D. Transmission Electron Microscopy

Microstructure analysis of the interface between thin films and substrates was performed by cross-sectional TEM. The samples for TEM were made by standard methods. They were glued together face-to-face with epoxy resin then mechanically polished to a thickness of approximately 100 μm, dimpled from one side to get a thickness of approximately 20 μm at the center, followed by ion milling using a Gatan precision ion polishing system. TEM investigations were carried out with a Jeol 1010 equipment operating at 100 keV.

3. Results and Discussion

A. Characterization of Al_2O_3 and TiO_2 Films

Al_2O_3 and TiO_2 thin films of 10 to 400 nm thickness were deposited in the 80 to 250 °C temperature range. The film thicknesses determined through ellipsometry were in excellent agreement with the TEM data. The growth rates of Al_2O_3 and TiO_2 were in the range of 1–1.25 and 0.3–0.7 Å′/cycle. Higher deposition rates were obtained when H_2O_2 was used as a precursor. The growth rates (g) did not depend significantly on the substrate material; however, the linear fit ($t = y + N * g$) of the film thickness (t) versus number of cycles (N) showed a considerable variation (up to 5 nm) for the y-intercept values between the substrates, indicating that the substrate material has a significant effect on the initial "seed" film. This effect is related to the incubation time of the coating process and is also temperature dependent. Depending on the substrate material and surface roughness, the precursor has a higher affinity and more precursor may adsorb on the surface to form a saturated monolayer. In subsequent cycles, the substrate influence on the adsorption is minimal.

The optical constants of the Al_2O_3 films have been parameterized by the Cauchy function with an extinction coefficient $k = 0$. The Cauchy, Lorenz, and Tauc–Lorenz formalisms have been applied to the analysis of the TiO_2 film thicknesses and optical constants. The Tauc–Lorenz formalism improved the ellipsometric fit and decreased the mean square error value. It yielded nonzero extinction coefficient below 400 nm, however, of the order of 10^{-3}, showing minimal absorbance of the deposited films. This value is in accordance with previously reported data [11] showing applications for optical filters in the 230–280 nm spectral range. Further analysis of the ALD coatings at shorter wavelengths is necessary to prove that these are of comparable quality and may also be used for such applications.

The experimental dispersion curves are depicted in Fig. 1. The Al_2O_3 refractive index has minimal dependence on the deposition temperature and shows low dispersion, with values of 1.65 ± 0.05 throughout the visible and NIR spectral range. In contrast, the TiO_2 refractive index at 633 nm increases from ~2.1 to ~2.5 with increasing substrate temperature from 80 to 200 °C. Similar behavior of the TiO_2 films was observed with other deposition techniques [4] and reported also for ALD films [12,13]. The TEM micrograph in Fig. 2 of a TiO_2/Al_2O_3 bilayer deposited at 120 °C shows that both films are amorphous. At higher temperature (>165 °C), the anatase phase is formed, and one can observe a relative increase of the refractive index (~0.15) for the films deposited around 150–200 °C compared with the 120 °C deposition [12]. Nonetheless, the optical constants of the

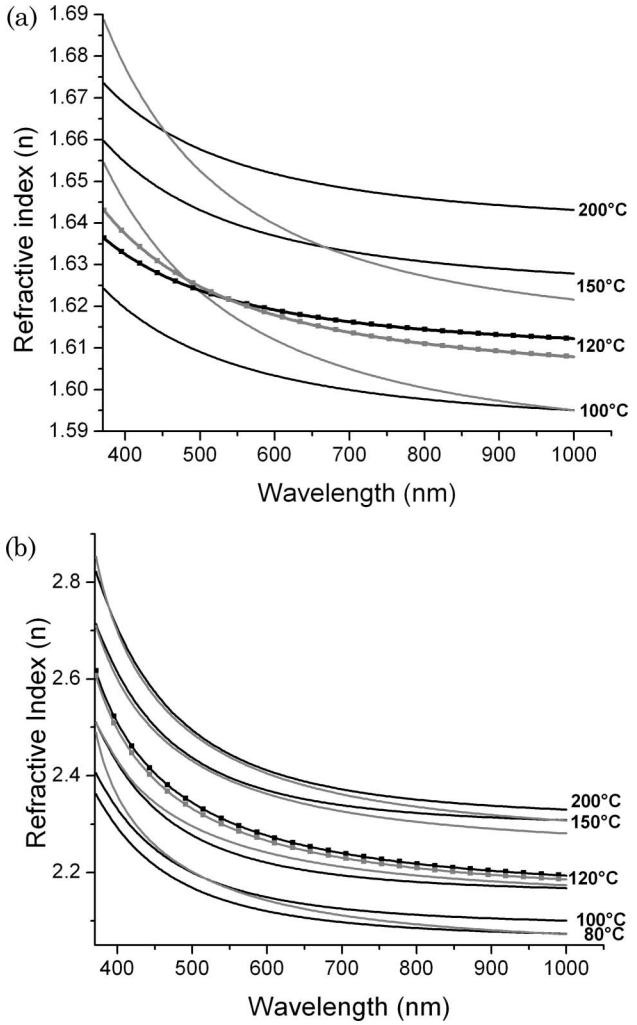

Fig. 1. Dispersion curves of (a) Al_2O_3 and (b) TiO_2 as functions of substrate temperature determined by spectroscopic ellipsometry. The black curves correspond to the refractive indices measured on the Si wafer, whereas the gray curves depict the corresponding data on BK7 glass. The ALD deposition was done with H_2O as precursor for oxygen source (plain curves) or H_2O_2 (curves with squares, shown only for 120 °C). Note the different scale of the refractive index.

films grown on Si wafer did not vary significantly from the ones on BK7 glass (~0.03).

B. Narrow Bandpass Filter

Using the refractive indices of alumina and titania determined for the ALD process employing H_2O_2, we designed a dichroic filter with a bandpass transmittance at 470 nm and FWHM of 4 nm. The filter is made of 15 layers of the $H(LH)^3(2L)(HL)^3H$ type, where H corresponds to high and L to low refractive index material. The corresponding target film thicknesses are 50.1 nm for H (TiO_2) and 72.4 nm for L (Al_2O_3). Theoretical modeling has shown that the bandpass wavelength can be shifted significantly through slight variation of the ($2L$) alumina film thickness. Figure 3 illustrates the color-coded transmittance of filters as function of this ($2L$) layer thickness. The calculations show that a thickness variation of the spacer alumina layer from 120 to 170 nm shifts the bandpass wavelength from 445 to 490 nm, while the FWHM is <5 nm.

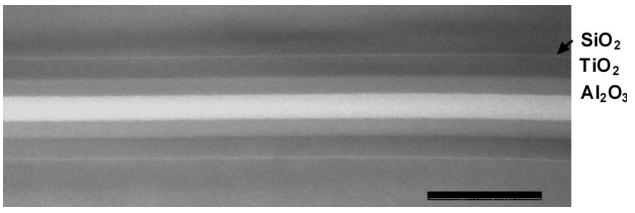

Fig. 2. TEM micrograph of a TiO_2/Al_2O_3 bilayer on the Si wafer. The native SiO_2 layer of ~1.5 nm can be observed. The scale bar is 200 nm.

Experimentally, we produced a set of five filters with various ($2L$) layer thicknesses. The layer thickness offset amounts ~6 nm corresponding to 50 cycles of Al_2O_3 deposition (up to ±12 nm deviation from the target thickness). Samples were successively removed from the reaction chamber and kept under standard laboratory conditions until the largest Al_2O_3 thickness was reached. Then the ALD process was concomitantly finished on all samples. Figure 4 depicts the transmittance spectra of the obtained dichroic filters. The wavelength position of the filters shifts from 469 to 485 nm with increasing thickness of the spacer ($2L$) layer as controlled by ALD. The calculated transmittance of the bandpasses reaches 92% with a sideband transmittance of 1–3%. The experimental peak transmittance measured at ~3 nm spectral resolution is in the 60–70% range.

The film thicknesses of the layers (15 variables) were determined through a fit to the transmittance spectra for each sample, whereas the optical constants were kept constant (see Table 1). The presence of the interference peaks in the NBPF samples make it possible to obtain an excellent fit to the experimental transmittance data. The calculated film thicknesses show some variation between samples for each layer. This nonuniformity is low and could be further reduced through optimization of the reaction chamber for optical coatings. Additionally, the bottom layers have a lower thickness than the corresponding upper ones, although the same number of cycles was applied indicating the influence of the seed material on the growth rate and possibly slight variation in the deposition conditions. Another explanation is possibly the formation of refractive index gradients at increasing film thicknesses as reported previously for TiO_2 [13].

The optical analysis of the NBPFs on a section of the samples coated on both sides of the substrate (without a mask) was carried out to assess the uniformity of the coating on the front and back sides. The transmittance spectra (see Fig. 5 for selected spectra of samples 1–3) show that a double-side coating nearly perfectly suppresses the transmittance peaks around 470 nm. Additional layers may be added to the coating sequence to enhance the transmittance above 600 nm and produce edge filters.

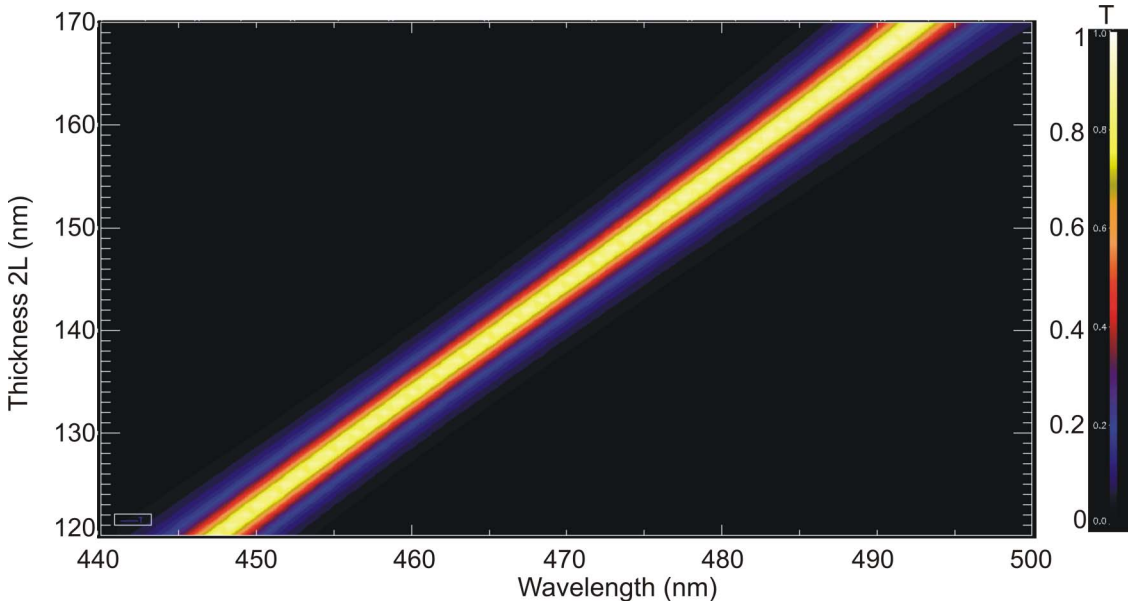

Fig. 3. (Color online) Calculated transmittance of the target NBPF as function of the ($2L$) layer thickness. The bandpass wavelength shifts to higher wavelength with increasing thickness.

Coating processes applied to dichroic filters require tight *in situ* control of the layer thickness and continuous process adjustment. Although in this ALD process no *in situ* measurement was applied, the target bandpass filter could be achieved, and the bandpass wavelength could be efficiently shifted to obtain a variety of filters. The capability of ALD to simultaneously coat both sides of the substrate with uniform films may offer additional advantages for producing NBPFs.

Recently, significant efforts were directed to develop commercially available ALD tools adapted to *in situ* ellipsometry monitoring. Although ALD tools equipped with quartz microbalance have been available, the optical (ellipsometric, transmittance/reflectance) control of the film thicknesses will reinforce the application of ALD for optical coatings. A significant advantage of ALD coating technology versus sputtering and ion-assisted deposition techniques is the capability of large batch reactor chambers (up to 1 m length, ~80 cm diameter are currently available). The uniformity of the ALD films is ~1–2%, even in such large coating chambers. Nonetheless, complex optical elements will require even more stringent control of the optical thicknesses to achieve the target function. Hence optical monitoring for each or several optical elements must be probably implemented during the ALD process to indentify turning points [10]. Once errors are identified, correction can be carried out in a perfectly controlled manner on an atomic scale by ALD. It may be also possible to develop ALD chambers with correction capability (i.e., process a few more cycles) for each optical element, such as by shielding the other optics. Alternatively, it may become attractive to combine ALD tools with faster (CVD, sputtering, PVD) equipment and use ALD for the extremely thin layers and for corrective purposes in the optical coating industry.

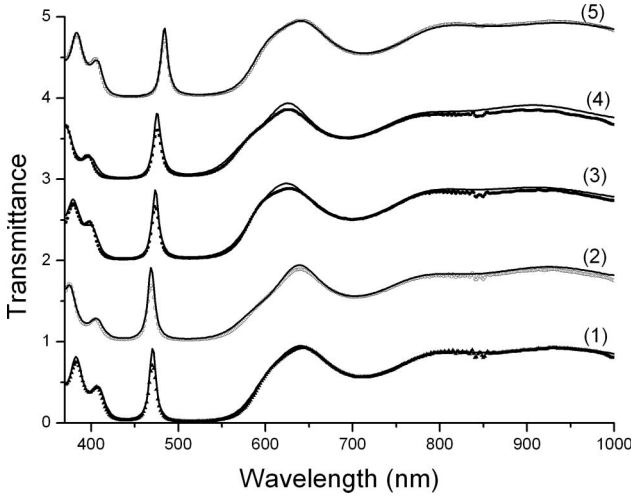

Fig. 4. Transmittance spectra of the NBPF optics of the five dichroic filters. The spectra are offset by one for clarity. The doted curves correspond to the experimental data, and the plain curves correspond to the calculated spectrum. The bandpass wavelength is shifted from 469 to 485 nm.

C. Antireflection Coating

Broadband antireflective coatings were deposited on PC, BK7 glass, and quartz substrates. The antireflective coatings are made of five alternating layers ($LHLHL$) where L corresponds to Al_2O_3 and H to TiO_2 with layer thicknesses in the range of 14 to 80 nm. Selected transmittance spectra are depicted in Fig. 6. The samples coated on both sides show above 98% transmittance. The antireflective coatings on the front and back sides improve the transmittance by 6–7% compared to uncoated substrates. The advantage of ALD over other coating technolo-

Table 1. Individual Layer Thicknesses of the Narrow-Bandpass Filter Samples Calculated through a Fit of the Transmittance Spectra (see Fig. 4)[a]

		Sample 1	Sample 2	Sample 3	Sample 4	Sample 5
Peak Position (nm)		470	469	473	477	485
Substrate		1.2 mm				
Layer	PC	Thickness (nm)				
1	TiO_2	41.9	43.5	39.9	45.2	43.4
2	Al_2O_3	68.1	63.7	66.6	69.6	61.2
3	TiO_2	47.2	45.3	46.2	45.7	45.4
4	Al_2O_3	72.3	69.2	70.4	74.4	67.7
5	TiO_2	50.5	46.0	47.3	48.7	43.1
6	Al_2O_3	78.1	74.8	77.2	78.2	75.2
7	TiO_2	54.6	55.5	59.9	52.0	53.6
8 (2*L*)	Al_2O_3	125.1	130.5	136.1	148.8	149.2
9	TiO_2	58.1	53.8	49.9	52.5	49.2
10	Al_2O_3	77.5	79.5	77.5	78.0	77.0
11	TiO_2	50.7	54.1	52.0	49.7	54.8
12	Al_2O_3	78.0	76.2	75.1	78.1	75.9
13	TiO_2	51.9	47.9	45.3	51.3	41.7
14	Al_2O_3	81.0	80.1	76.8	79.3	75.5
15	TiO_2	57.4	60.6	61.9	55.8	62.6

[a]The variable parameters total 15 layer thicknesses.

gies is that the film deposition occurs on both sides simultaneously, and therefore the coating time is reduced. Single-side-coated samples were obtained with a protection mask. The transmittance of these samples is improved by 3–4% compared to the uncoated substrates.

The transmittance of the uncoated substrates (PC 88%, BK7 92%, quartz 92% at 500 nm) will affect the transmittance of the coated samples. The transmittance at 500 nm of the double-side-coated PC reaches ~94% while coated BK7 and quartz show ~96% transmittance at this wavelength. Figure 6 shows that the coating on the PC substrate produced an increased transmittance toward the UV VIS region (400–550 nm), while the deposition on the BK7 and quartz samples produced highest transmittance in the VIS IR region, although the PC and BK7 samples were coated simultaneously, and the quartz samples several months later. As mentioned in Subsection 3.A, the film thickness will also depend on the substrate material. The coating parameters were optimized for the BK7 substrate because of considerable difficulty in determining the optical constants and growth rates on PC and quartz.

ALD allows the antireflective coating of complex and high aspect ratio substrates. Hence such antire-

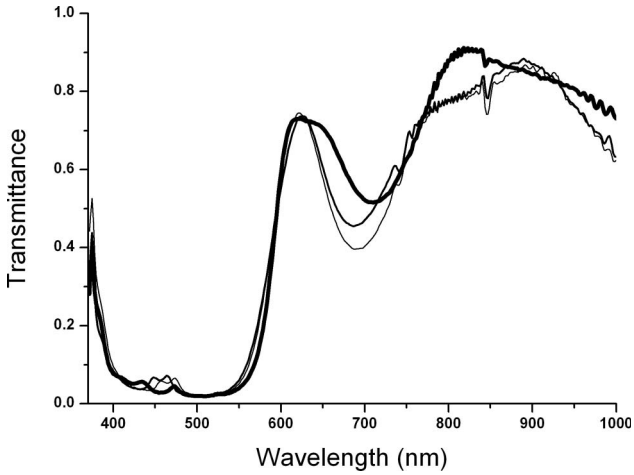

Fig. 5. Selected transmittance spectra of the NBPF optics [samples 1 (thick curve), 2 (medium curve), and 3 (thin curve)] recorded from a portion of the substrate where the coating has been applied on both sides. Such coatings would be an approach to produce edge filters.

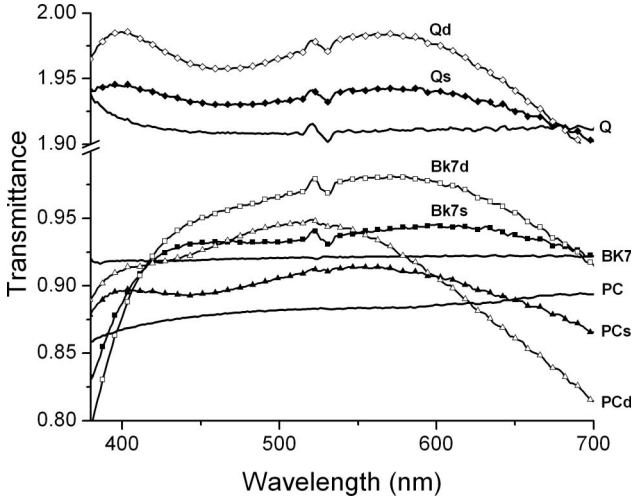

Fig. 6. Transmittance spectra of the antireflective coating samples. The uncoated reference spectra (plain curve) are included for PC, BK7 glass (BK7), and quartz (Q). The single-side coating is depicted by "s" and filled symbols, and the double-side coating is depicted by "d" and open symbols. The spectra of the quartz samples are offset by one for clarity.

flective coatings are promising for optics with curved surfaces, such as lenses and microarrays, without additional mechanical repositioning of the samples to achieve uniform coating. The excellent film thickness control of ALD makes it possible to deposit very thin layers (<20 nm) without *in situ* control. Since several precursors can be connected simultaneously to the ALD equipment, there is no delay in depositing the next layer of a different material. Through the ALD control, there is no mixing of the layer materials, and the layer transition is sharp. Hence, although the grow rate in ALD is relatively low compared to other coating techniques, the total deposition time can be minimized.

4. Conclusions

ALD is a promising technique for producing high-quality optical coatings on various substrates. Antireflective coatings and NBPFs can be realized if a detailed knowledge of the optical properties and growth rates of the materials are available. The capability of ALD to simultaneously coat both surfaces of the substrate may be used in the design of the optical elements, providing considerable advantage over other coating technologies. Improvement of the optical elements and design may be possible using lower refractive index materials. Characterization of optical coating materials in the deep UV spectral range is in progress to broaden the application field of ALD.

Financial support of the Bundesministerium für Bildung und Forschung (BMBF) (project FKZ 13N9711) is highly acknowledged. The authors are thankful to S. Hopfe for TEM sample preparation.

References

1. U. Schulz, U. B. Schallenberg, and N. Kaiser, "Antireflection coating for plastic optics," Appl. Opt. **41**, 3107–3110 (2002).
2. V. Janicki, D. Gäbler, S. Wilbrandt, R. Leitel, O. Stenzel, N. Kaiser, M. Lappschies, B. Görtz, D. Ristau, C. Rickers, and M. Vergöhl, "Deposition and spectral performance of an inhomogeneous broadband wide-angular antireflective coating," Appl. Opt. **45**, 7851–7857 (2006).
3. M. Yang, A. Gatto, and N. Kaiser, "Design and deposition of vacuum-ultraviolet narrow-bandpass filters for analytical chemistry applications," Appl. Opt. **45**, 1359–1363 (2006).
4. F. Flory and L. Escouba, "Optical properties of nanostructured thin films," Prog. Quantum Electron. **28**, 89–112 (2004).
5. H. Takashashi, "Temperature stability of thin-film narrow-bandpass filters produced by ion-assisted deposition," Appl. Opt. **34**, 667–675 (1995).
6. M. Knez, K. Nielsch, and L. Niinistö, "Synthesis and surface engineering of complex nanostructures by atomic layer deposition," Adv. Mater. **19**, 3425–3438 (2007).
7. D. Riihelä, M. Ritala, R. Matero, and M. Leskel, "Introducing atomic layer epitaxy for the deposition of optical thin films," Thin Solid Films **289**, 250–255 (1996).
8. R. R. Willey, "Simulation of errors in the monitoring of narrow bandpass filters," Appl. Opt. **41**, 3193–3195 (2002).
9. R. R. Willey, "Monitoring thin films of the fence post design and its advantages for narrow bandpass filters," Appl. Opt. **47**, C147–C150 (2008).
10. R. R. Willey, *Practical Design and Production of Optical Thin Films* (Marcel Dekker, 2002).
11. J. H. Correia, A. R. Emadi, and R. F. Wolffenbuttel, "UV bandpass optical filter for microspectrometers," ECS Transactions **4**, 141–147 (2006).
12. J. Aarik, A. Aidla, A. A. Kiisler, T. Uustare, and W. Sammelselg, "Effect of crystal structure of TiO_2 films grown by atomic layer deposition," Thin Solid Films **305**, 270–273 (1997).
13. A. Kasikov, J. Aarik, H. Mändar, M. Moppel, M. Pärs, and U. Uustare, "Refractive index gradients in TiO_2 thin films grown by atomic layer deposition," J. Phys. D **39**, 54–60 (2006).